MIT Libraries | DSpace@MIT

MIT Open Access Articles

Enhancement of thermoelectric figure-of-merit at low temperatures by titanium substitution for hafnium in n-type half-Heuslers Hf[subscript0.75−x]Ti[subscript x]Zr[subscript 0.25]NiSn[subscript 0.99]Sb[subscript 0.01]

Massachusetts Institute of Technology

Enhancement of thermoelectric figure-of-merit at low temperatures by Titanium substitution for Hafnium in *n*-type half-Heuslers Hf$_{0.75-x}$Ti$_x$Zr$_{0.25}$NiSn$_{0.99}$Sb$_{0.01}$

Giri Joshi[1], Tulashi Dahal[1], Shuo Chen[1], Hengzhi Wang[1], Junichiro Shiomi[2], Gang Chen[3*], and Zhifeng Ren[1*]

[1] Department of Physics, Boston College, Chestnut Hill, Massachusetts 02467, USA

[2] Department of Mechanical Engineering, The University of Tokyo, 7-3-1 Hongo, Bunkyo-ku, Tokyo, 113-8656, Japan

[3] Department of Mechanical Engineering, Massachusetts Institute of Technology, Cambridge, Massachusetts 02139, USA

Abstract

The effect of titanium (Ti) substitution for hafnium (Hf) on thermoelectric properties of (Hf,Zr)-based *n*-type half-Heuslers: Hf$_{0.75-x}$Ti$_x$Zr$_{0.25}$NiSn$_{0.99}$Sb$_{0.01}$, has been studied. The samples are made by arc-melting followed by ball milling and hot pressing via the nanostructuring approach. A peak thermoelectric figure-of-merit (*ZT*) of ~1.0 is achieved at 500 ^{o}C in samples with a composition of Hf$_{0.5}$Zr$_{0.25}$Ti$_{0.25}$NiSn$_{0.99}$Sb$_{0.01}$ due to a slight increase in carrier concentration and also a lower thermal conductivity caused by Ti. The *ZT* values below 500 ^{o}C of hot pressed Hf$_{0.5}$Zr$_{0.25}$Ti$_{0.25}$NiSn$_{0.99}$Sb$_{0.01}$ samples are significantly higher than those of the same way prepared Hf$_{0.75}$Zr$_{0.25}$NiSn$_{0.99}$Sb$_{0.01}$ samples at each temperature, which is very much desired for mid-range temperature applications such as waste heat recovery in automobiles.

*Corresponding authors: gchen2@mit.edu and renzh@bc.ed

I. Introduction

Half-Heuslers (HHs) have great potential to convert waste heat into electricity through thermoelectric effect in the medium (200-500 $^{\circ}$C) and high (500-700 $^{\circ}$C) temperature range [1]. HH phases are intermetallic, complex compounds (in general they have MM'X chemical formula, where M is Ti or Zr or Hf or a combination of two or all three, M' is Co or Ni, and X is Sn or Sb) that crystallize in cubic crystal structure of the *F4/3m* (No. 216) space group. These phases are well-known semiconductors with 18 valence electrons per unit cell, which have higher Seebeck coefficient with moderate electrical conductivity due to a narrow energy gap [2-6]. Since the performance of the thermoelectric materials directly depends on the dimensionless figure-of-merit (*ZT*), defined as $(S^2\sigma/\kappa)T$ [7], where S is the Seebeck coefficient, σ the electrical conductivity, κ the thermal conductivity, and T the absolute temperature. HHs could be a good thermoelectric material due to their higher power factor ($S^2\sigma$) [8,9]. In the past few years, experiments have shown that MNiSn and MCoSb phases exhibit promising *n*- and *p*-type thermoelectric properties, respectively [8,9]. However, the *ZT* of the HHs are much lower to compete with the state-of-the-art thermoelectric materials [10,11] due to their relatively higher thermal conductivity [8,9]. In the recent years, different approaches have been used to improve the *ZT* of HH compounds such as optimization of the composition [12-18] and introduction of nanostructures by a nanostructuring approach [19,20], and peak *ZT*s of ~0.8 for *p*-type [19] and ~1.0 for *n*-type [20,21] at around 700 $^{\circ}$C has been reported in (Hf,Zr) based nanostructured HHs. Alloy effect has been useful to decrease the thermal conductivity in many thermoelectric materials. Building on our success of achieving good *ZT*s in *p*-type $Hf_{0.5}Zr_{0.5}CoSb_{0.8}Sn_{0.2}$ [19] and *n*-type $Hf_{0.75}Zr_{0.25}NiSn_{0.99}Sb_{0.01}$ [20], we studied the effect of partial substitution of Hf with Ti on thermoelectric properties expecting to have lower thermal conductivity due to the larger

2

atomic mass and size differences of Hf and Ti than that of Hf and Zr. In fact, the benefit of the larger atomic mass and size differences of Hf and Ti than that of Hf and Zr in p-type HH has recently been demonstrated [22]. Here we show a decent improvement in ZT in the range of 100-500 ^{o}C, with a peak ZT of ~1.0 at 500 ^{o}C by partial replacement of Hf with Ti in the reported best n-type composition $Hf_{0.75}Zr_{0.25}NiSn_{0.99}Sb_{0.01}$ through nanostructuring approach by ball milling and hot pressing [10,19,20,22,23}. The ZT improvement at lower temperatures and the shift in peak ZT benefit from the change in carrier concentration and mobility caused by the partial substitution of Ti for Hf and the reduction of thermal conductivity due to alloy scattering effect.

Even though the peak ZT remains comparable with the previously reported result of the samples prepared in the same way [20], the ZT values at lower temperatures are higher, which results in a higher average ZT below 500 ^{o}C. Such a higher average ZT is very much desired for medium temperature applications such as waste heat recovery in vehicles where the exhaust gas temperature is usually less than 600 ^{o}C.

II. Experimental

Nanostructured half-Heusler compounds were prepared by arc melting hafnium (Hf) (99.99%, Alfa Aesar), titanium (Ti) (99.99%, Alfa Aesar), and zirconium (Zr) (99.99%, Alfa Aesar) chunks with nickel (Ni) (99.99%, Alfa Aesar), tin (Sn) (99.99%, Alfa Aesar), and antimony (Sb) (99.99%, Alfa Aesar) pieces according to the required composition (Hf,Ti,Zr)Ni(Sn,Sb). Then the melted ingot was ball milled for 5-20 hours to get the desired nanopowders. The mechanically prepared nanopowders were then pressed at temperatures of

1000-1050 °C by a dc hot pressing method in graphite dies with a 12.7 mm central cylindrical opening diameter to get bulk dense nanostructured half-Heusler samples.

The hot pressed dense bulk samples were characterized by X-ray diffraction (XRD D8 Discover Model) and transmission electron microscopy (TEM, JEOL 2010F) to study their crystallinity, composition, the average grain size, and grain size distribution. These parameters significantly affect the thermoelectric properties of the final dense bulk samples.

The hot pressed dense bulk nanostructured samples were then cut into 2 mm × 2 mm × 12 mm bars for electrical conductivity and Seebeck coefficient measurements, 12.7 mm diameter discs with appropriate thickness for thermal diffusivity and Hall coefficient measurements, and 6 mm diameter discs with appropriate thickness for specific heat capacity measurements. The electrical conductivity and Seebeck coefficient were measured by commercial equipment (ZEM-3, Ulvac), the thermal diffusivity was measured by a laser flash system (LFA 457, Netzsch) from room temperature to 700 °C, the carrier concentration and mobility at room temperature were acquired from Hall measurements (Lakeshore 7600), and the specific heat capacity was measured on a differential scanning calorimeter (200-F3, Netzsch). The thermal conductivity was calculated as the product of the thermal diffusivity, specific heat capacity, and volumetric density of the samples. The volumetric densities of hot pressed samples are 9.73, 9.01, 8.17, and 7.34 g/cm^3 measured using an Archimedes' kit for $Hf_{0.75-x}Ti_xZr_{0.25}NiSn_{0.99}Sb_{0.01}$ with x = 0, 0.25, 0.5, and 0.75, respectively, corresponding to 98.5% (9.87 g/cm^3), 99.8% (9.03 g/cm^3), 99.3% (8.23 g/cm^3), and 100% (7.34 g/cm^3) of the theoretical densities of each composition calculated from their crystal structures.

III. Results and Analyses

4

In this section, we discuss the effects of Ti substitution on thermoelectric properties of (Hf,Zr) based n-type HH. The basic purpose of choosing Ti substitution is to increase the effect of larger atomic mass and size differences of Hf and Ti than that of Hf and Zr on stronger alloy scattering of phonons, which could significantly change the thermoelectric properties of the materials. Here, we present the characterization and thermoelectric properties of hot pressed dense bulk samples $Hf_{0.75-x}Ti_xZr_{0.25}NiSn_{0.99}Sb_{0.01}$ (x = 0, 0.25, 0.5, and 0.75) prepared through the arc melting, ball milling, and hot pressing process [19,20]. For better readability, we chose not to present the individual properties of the composition with x = 0.75 in Figure 3.

Figure 1 shows the XRD patterns (Fig. 1a) and lattice constants (Fig. 1b) of the hot pressed dense bulk samples $Hf_{0.75-x}Ti_xZr_{0.25}NiSn_{0.99}Sb_{0.01}$ (x = 0, 0.25, 0.5, and 0.75). Figure 1a clearly shows that the XRD patterns of all compositions are similar demonstrating similar grain sizes since the broadening of the peaks of hot pressed samples is only due to the grain size effect, and the peaks are well matched with those obtained for half-Heusler phases (Fig. 1a) [17]. Moreover, the lattice constant calculated from XRD peaks decreases according to Vegards Law with increasing the titanium concentration. The calculated lattice constant of TiNiSn from Figure 1b is around 5.945 Å, which is close to the literature value [24].

To confirm the effect of Ti substitution on grain size, TEM study of hot pressed dense bulk samples $Hf_{0.75-x}Ti_xZr_{0.25}NiSn_{0.99}Sb_{0.01}$ (x = 0 and 0.25) has been performed. Figure 2 shows the TEM images of the hot pressed samples of $Hf_{0.75}Zr_{0.25}NiSn_{0.99}Sb_{0.01}$ (Figs. 2a & b) and $Hf_{0.5}Ti_{0.25}Zr_{0.25}NiSn_{0.99}Sb_{0.01}$ (Figs. 2c & d) compositions. The contrasts in the TEM images are the results of different crystalline orientations of different grains in the samples. Since the polycrystalline samples are prepared by hot pressing of ball milled powders, the grain orientations are random. Under the irradiation of electron beam, the grains that are close to

Bragg's diffraction condition strongly diffract the electrons. As we are collecting transmission electrons for imaging, these grains appear darker than those grains deviating from Bragg's diffraction condition. Figures 2 clearly shows that the hot pressed dense bulk samples of both $Hf_{0.75}Zr_{0.25}NiSn_{0.99}Sb_{0.01}$ (Figs. 2a) and $Hf_{0.5}Ti_{0.25}Zr_{0.25}NiSn_{0.99}Sb_{0.01}$ compositions (Fig. 2c) contain the grains of around 200 – 300 nm showing no difference in grain size due to Ti substitution. Figure 2 also shows that the grain boundaries and crystallinity of both samples are similar (Figs. 2b & d).

Figures 3 show the temperature dependent electrical conductivity (Fig. 3a), Seebeck coefficient (Fig. 3b), thermal diffusivity (Fig. 3c), specific heat capacity (Fig. 3d), thermal conductivity (Fig. 3e), and *ZT* (Fig. 3f) of hot pressed dense bulk nanostructured samples $Hf_{0.75-x}Ti_xZr_{0.25}NiSn_{0.99}Sb_{0.01}$ (x = 0.25, 0.5, and 0.75, for better readability of the figure, we chose not to present the individual data of composition with x = 0.75) in comparison with the previously reported (Hf,Zr)-based best *n*-type half-Heusler composition ($Hf_{0.75}Zr_{0.25}NiSn_{0.99}Sb_{0.01}$) prepared under the same conditions by the same method of arc melting, ball milling, and hot pressing process [20]. Figures 3a clearly shows that the electrical conductivity decreases at first and then increases with the increase of Ti concentration (Inset of Fig. 3a). The decrease should be due to the effect of alloy scattering of charge carriers to decrease the mobility (shown later in Fig. 4), and the increase may be related to electronic band structure due to too much Ti when x = 0.75. The Seebeck coefficient follows the opposite trend of electrical conductivity (Fig. 3b). However, the thermal diffusivity of Ti substituted samples [$Hf_{0.75-x}Ti_xZr_{0.25}NiSn_{0.99}Sb_{0.01}$ (x = 0.25 and 0.5)] is significantly lower than that of $Hf_{0.75}Zr_{0.25}NiSn_{0.99}Sb_{0.01}$ composition (Fig. 3c). Even though the specific heat capacity increases with increasing Ti content (Fig. 3d) due to smaller atomic mass, the thermal conductivity of Ti substituted samples decreases significantly in

comparison with $Hf_{0.75}Zr_{0.25}NiSn_{0.99}Sb_{0.01}$ sample prepared in the same way (Fig. 3e). As a result, the *ZT* values are much more improved at lower temperatures (100 – 500 ^{o}C) with a peak *ZT* of ~1.0 at 500 ^{o}C in $Hf_{0.5}Ti_{0.25}Zr_{0.25}NiSn_{0.99}Sb_{0.01}$ composition in comparison with the previously reported (Hf,Zr)-based best *n*-type half-Heusler composition ($Hf_{0.75}Zr_{0.25}NiSn_{0.99}Sb_{0.01}$) (Fig. 3f) [20]. The improvement in *ZT* at lower temperatures could be beneficial for medium (200 – 500 ^{o}C) temperature applications such as waste heat recovery in vehicles.

Figure 4 shows the room temperature carrier concentration and mobility of the hot pressed dense bulk nanostructured samples $Hf_{0.75-x}Ti_xZr_{0.25}NiSn_{0.99}Sb_{0.01}$ (x =0, 0.25, 0.5, and 0.75). It clearly shows that the behaviors of electrical conductivity (Fig. 3a) and Seebeck coefficient (Fig. 3b) in $Hf_{0.75-x}Ti_xZr_{0.25}NiSn_{0.99}Sb_{0.01}$ (x = 0.25, 0.5, and 0.75) compositions are due to the increase in carrier concentration and decrease in mobility with the Ti concentration. The increase in carrier concentration with Ti concentration (Fig. 4) could be possibly due to the change in electronic band structure, and the decrease in mobility could be due to the increase in alloy scattering of charge carriers. To gain insight into the influence of Ti substitution on electronic states, the density of states of two extreme cases TiNiSn and HfNiSn were calculated by the density functional theory under generalized gradient approximation for the electron exchange correlation potential with projector-augmented-wave pseudopotentials [24]. The results showed that TiNiSn, although its band gap is slightly larger than HfNiSn, has significantly higher density of states near the conduction band edge, which seems consistent with the experimental observation of carrier concentration increase with Ti concentration.

IV. Conclusions

7

Thermoelectric properties of (Ti,Zr,Hf)-based n-type half-Heuslers have been studied by using a nanostructuring approach, and a peak ZT of ~1.0 is observed at 500 $^{\circ}$C in hot pressed dense bulk nanostructured $Hf_{0.5}Zr_{0.25}Ti_{0.25}NiSn_{0.99}Sb_{0.01}$ samples. The lower concentration of Hf reduces the overall cost of the material due to the much higher cost of Hf than Ti. The nanostructured samples are initially prepared by ball milling and hot pressing of arc melted samples. The peak ZT value did not increase but shifted to a lower temperature meaning that the ZT values are much improved at lower temperatures, which could be very significant for medium temperature applications such as waste heat recovery in automobiles.

Reference

[1] S. J. Poon, Recent Trends in Thermoelectric Materials Research II, Semiconductors and Semimetals, edited by T. M. Tritt (2001), New York, p. 37.

[2] J. Tobola, J. Pierre, S. Kaprzyk, R. V. Skolozdra, M. A. Kouacou, J. Phys.: Condens. Matter 10 (1998), 1013.

[3] S. Ogut, K. M. Rabe, Phys. Rev. B 51 (1995), 10443.

[4] J. Tobola, J. Pierre, J. Alloys Compd. 296 (2000), 243.

[5] P. Larson, S. D. Mahanti, J. M. Kanatzidis, Phys. Rev. B 62 (2000), 12754.

[6] B. R. K. Nanda, I. Dasgupta, J. Phys.: Condens. Matter 15 (2003), 7307.

[7] D. M. Rowe, (Eds.) CRC Handbook of Thermoelectrics (1995), Boca Raton.

[8] Q. Shen, L. Chen, T. Goto, T. Hirai, J. Yang, G. P. Meisner, C. Uher, Appl. Phys. Lett. 79 (2001), 4165.

[9] Y. Xia, S. Bhattacharya, V. Ponnambalam, A. L. Pope, S. J. Poon, T. M. Tritt, J. Appl. Phys. 88 (2000), 1952.

[10]   B. Poudel, Q. Hao, Y. Ma, Y. C. Lan, A. Minnich, B. Yu, X. Yan, D. Z. Wang, A. Muto, D. Vashaee, X. Y. Chen, J. M. Liu, M. S. Dresselhaus, G. Chen, Z. F. Ren, Science 320 (2008), 634.

[11]   J. P. Fleurial, T. Caillat and A. Borshchevsky, In proceeding of the 13th International Conference on Thermoelectrics (1994), pp. 40-44.

[12]   J. Callaway, H. C. Von Baeyer, Phys. Rev. 120 (1960), 1149.

[13]   B. C. Sales, D. Mandrus, R. K. Williams, Science 272 (1996), 1325.

[14]   J. Yang, G. P. Meisner, L. D. Chen, Appl. Phys. Lett. 85 (2004), 1140.

[15]   L. D. Chen, X. Y. Huang, M. Zhou, X. Shi, W. B. Zhang, J. Appl. Phys. 99 (2006), 064305.

[16]   S. R. Culp, S. J. Poon, N. Hickman, T. M. Tritt, J. Blumm, Appl. Phys.Lett. 88 (2006), 042106.

[17]   T. Wu, W. Jiang, X. Y. Li, Y. F. Zhou, L. D. Chen, J. Appl. Phys. 102 (2007), 103705.

[18]   S. R. Culp, J. W. Simonson, S. J. Poon, V. Ponnambalam, J. Edwards, T. M. Tritt, Appl. Phys. Lett. 93 (2008), 022105.

[19]   X. Yan, G. Joshi, W. Liu, Y. Lan, H. Wang, S. Lee, J. W. Simonson, S. J. Poon, T. M. Tritt, G. Chen, Z. F. Ren, Nanoletters 11 (2011), 556.

[20]   G. Joshi, X. Yan, H. Wang, W. Liu, G. Chen, Z. F. Ren, Adv. Energy Mater. 1 (2011), 643.

[21]   S. J. Poon, D. Wu, S. Zhu, W. J. Xie, T. M. Tritt, P. Thomas, R. Venkatasubramanian, J. Mater. Res. 26 (2011), 2795.

[22]   X. Yan, W. S. Liu, H. Wang, S. Chen, J. Shiomi, K. Esfarjani, H. Z. Wang, D. Z. Wang, G. Chen, Z. F. Ren, Energy and Environmental Science 5 (2012), 7543.

[23]   G. Joshi, H. Lee, Y. C. Lan, X. W. Wang, G. H. Zhu, D. Z. Wang, R. W. Gould, D. C. Cuff, M. Tang, M. S. Dresselhaus, G. Chen, Z. F. Ren, Nanoletters 8 (2008), 4670.

[24]   J. Yang, H. Li, T. Wu, W. Zhang, L. Chen, J. Yang, Adv. Funct. Mater. 18 (2008), 2880.

Figure captions

Fig. 1 XRD patterns (Fig. 1a) and lattice constants (Fig. 1b) of hot pressed dense bulk nanostructured samples $Hf_{0.75-x}Ti_xZr_{0.25}NiSn_{0.99}Sb_{0.01}$ (x = 0, 0.25, 0.5, and 0.75).

Fig. 2 TEM images of hot pressed dense bulk nanostructured samples $Hf_{0.75}Zr_{0.25}NiSn_{0.99}Sb_{0.01}$ (Figs. 2a & b) and $Hf_{0.5}Ti_{0.25}Zr_{0.25}NiSn_{0.99}Sb_{0.01}$ (Figs. 2c & d).

Fig. 3 Temperature dependent electrical conductivity (Fig. 3a), Seebeck coefficient (Fig. 3b), thermal diffusivity (Fig. 3c), specific heat capacity (Fig. 3d), thermal conductivity (Fig. 3e), and *ZT* (Fig. 3f) of hot pressed dense bulk nanostructured samples $Hf_{0.75-x}Ti_xZr_{0.25}NiSn_{0.99}Sb_{0.01}$ (x = 0.25, and 0.5) in comparison with our previously reported best *n*-type half-Heusler sample $Hf_{0.75}Zr_{0.25}NiSn_{0.99}Sb_{0.01}$ free of Ti prepared in the same way by the same method [20].

11

Fig. 4 Carrier concentration and mobility of hot pressed dense bulk nanostructured samples $Hf_{0.75-x}Ti_xZr_{0.25}NiSn_{0.99}Sb_{0.01}$ (x = 0, 0.25, 0.5, and 0.75) at room temperature.
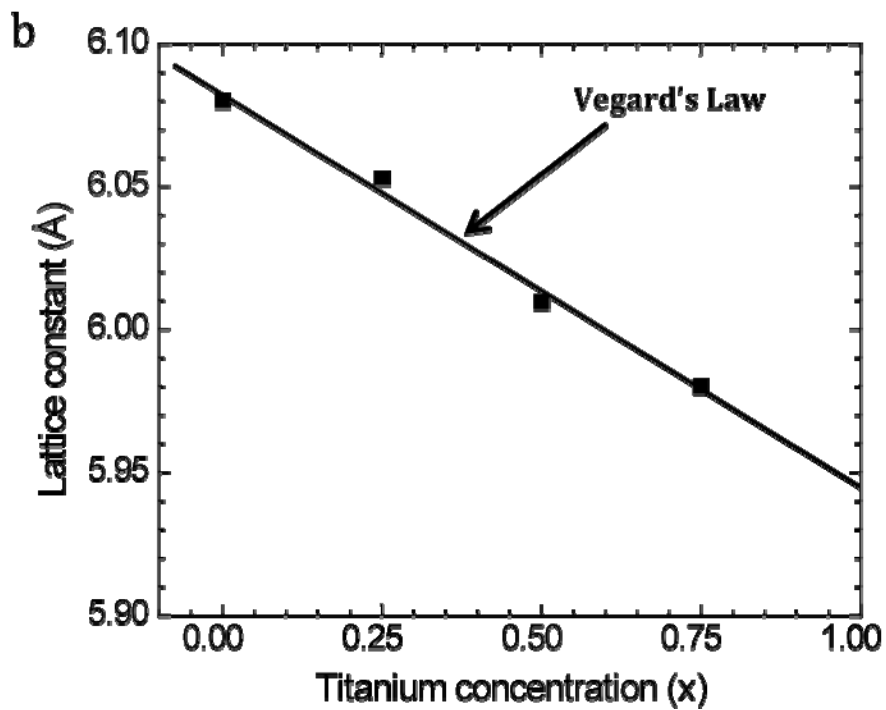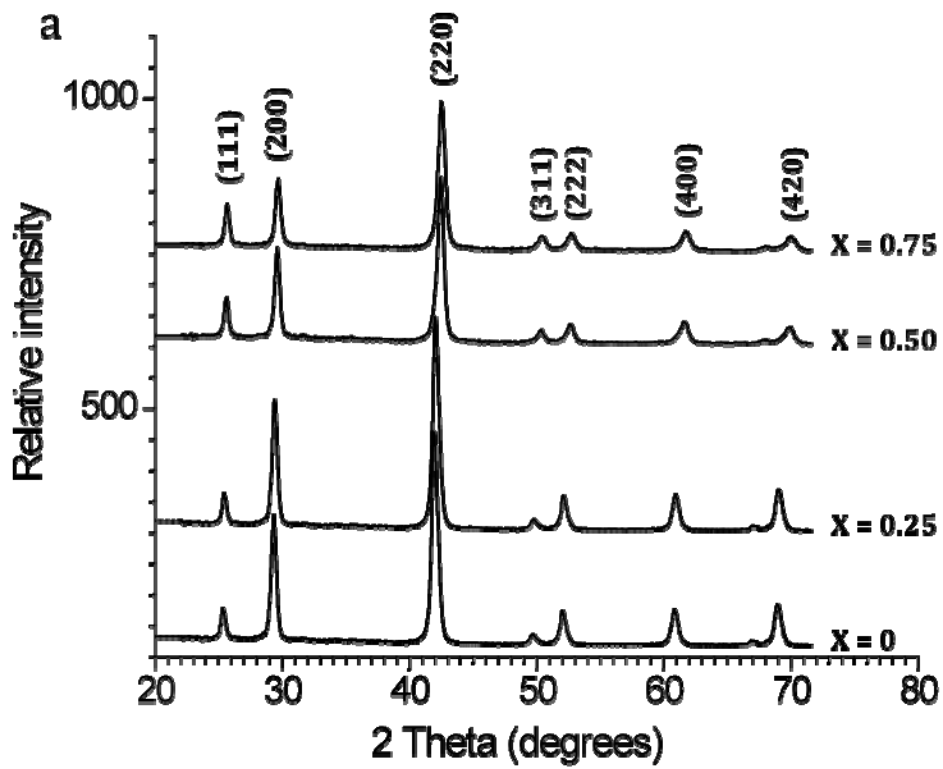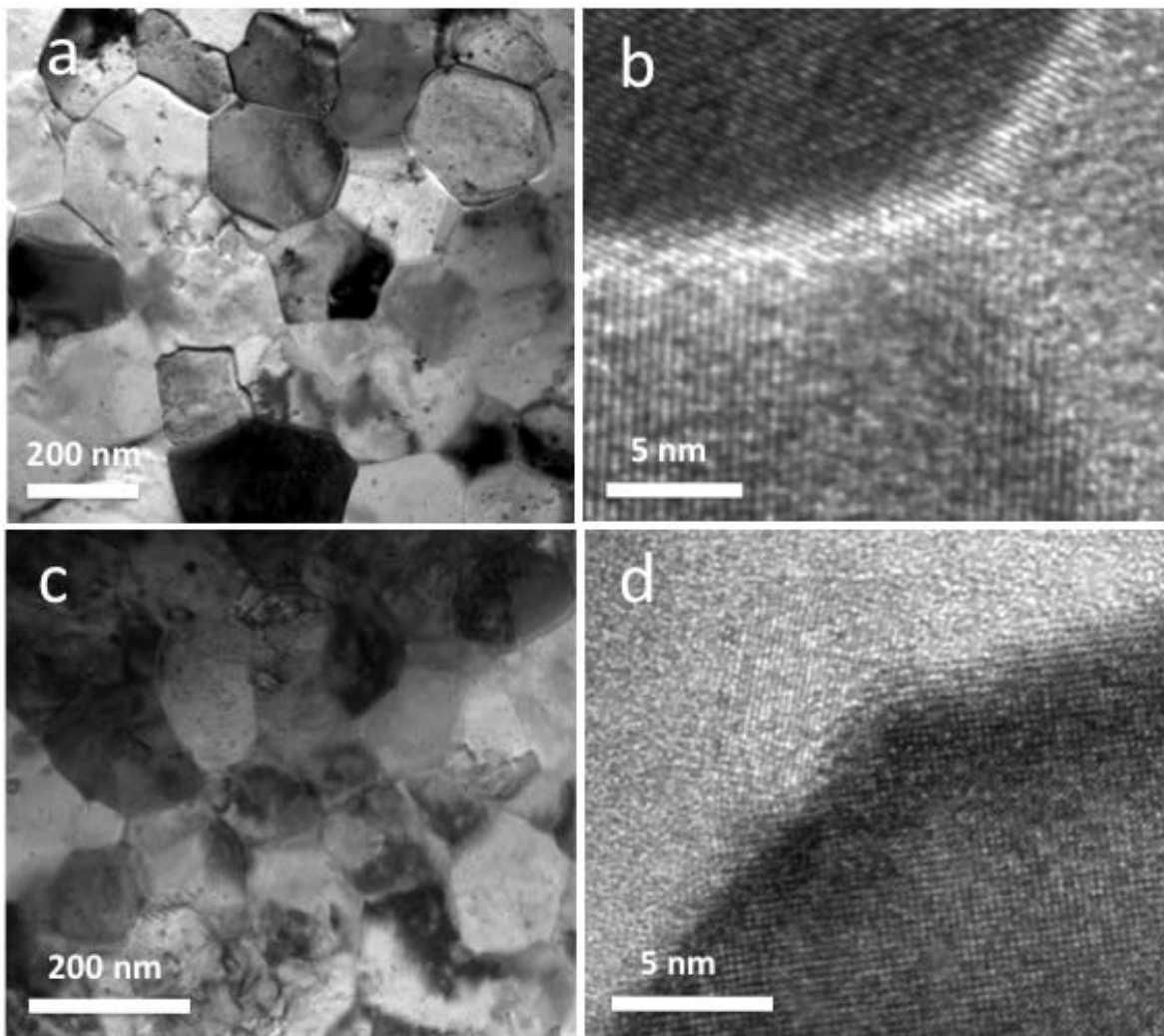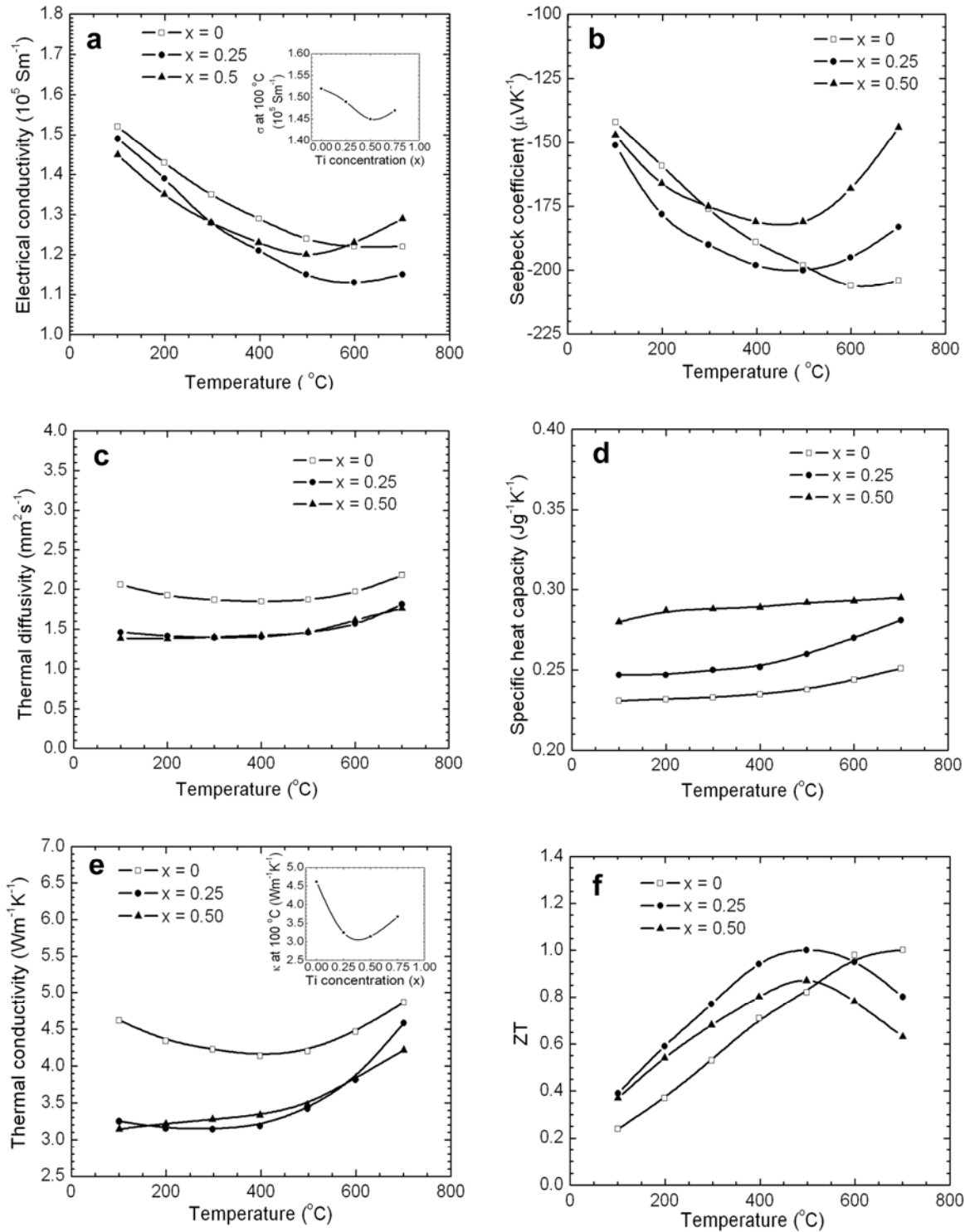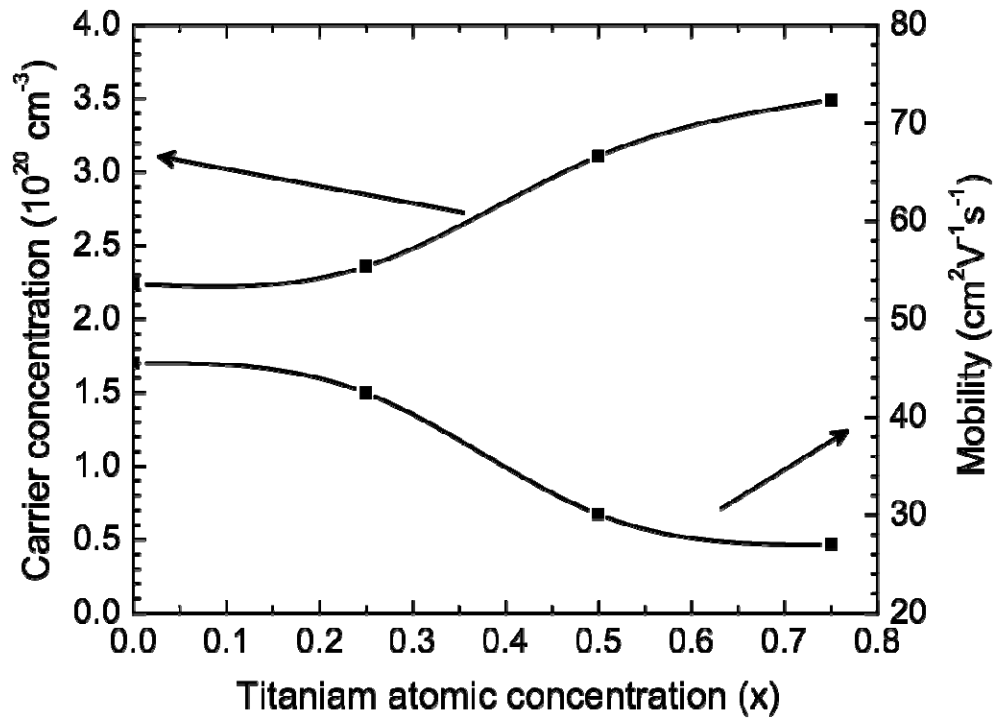
Figure 1. G. Joshi *et al.*

Figure 2. G. Joshi *et al.*

Figure 3. G. Joshi *et al*

Figure 4. G. Joshi *et al.*